JOURNAL OF BACTERIOLOGY, Oct. 2010, p. 4868–4875 Vol. 192, No. 19
0021-9193/10/$12.00 doi:10.1128/JB.00550-10

Different Roles of DosS and DosT in the Hypoxic Adaptation of Mycobacteria[▽]

Min-Ju Kim,[1] Kwang-Jin Park,[1] In-Jeong Ko,[2] Young Min Kim,[3] and Jeong-Il Oh[1]*

Department of Microbiology, Pusan National University, 609-735 Busan, South Korea[1]; Korea Science Academy of KAIST, 614-822 Busan, South Korea[2]; and Department of Biology, Yonsei University, 120-749 Seoul, South Korea[3]

Received 13 May 2010/Accepted 22 July 2010

The DosS (DevS) and DosT histidine kinases form a two-component system together with the DosR (DevR) response regulator in *Mycobacterium tuberculosis*. DosS and DosT, which have high sequence similarity to each other over the length of their amino acid sequences, contain two GAF domains (GAF-A and GAF-B) in their N-terminal sensory domains. Complementation tests in conjunction with phylogenetic analysis showed that DevS of *Mycobacterium smegmatis* is more closely related to DosT than DosS. We also demonstrated *in vivo* that DosS and DosT of *M. tuberculosis* play a differential role in hypoxic adaptation. DosT responds to a decrease in oxygen tension more sensitively and strongly than DosS, which might be attributable to their different autooxidation rates. The different responsiveness of DosS and DosT to hypoxia is due to the difference in their GAF-A domains accommodating the hemes. Multiple alignment analysis of the GAF-A domains of mycobacterial DosS (DosT) homologs and subsequent site-directed mutagenesis revealed that just one substitution of E87, D90, H97, L118, or T169 of DosS with the corresponding residue of DosT is sufficient to convert DosS to DosT with regard to the responsiveness to changes in oxygen tension.

Oxygen sensing is important for facultative anaerobes to adapt to changes in metabolic necessities during the transition between aerobic and anaerobic conditions. Although *Mycobacterium tuberculosis* (MTB) is an obligate aerobe, a gradual depletion of O_2 from its culture is known to lead to a drastic change in gene expression (8, 21, 24, 28, 34, 37, 39). Approximately 48 genes of *M. tuberculosis* were reported to be induced under early hypoxic conditions, which is mediated by the DosSR (DevSR) two-component system (16, 24, 34). The induction of the DosR regulon is important for survival of *M. tuberculosis* under hypoxic conditions and for it to enter the nonreplicating dormant state (2, 19). The DosSR two-component system consists of the DosS histidine kinase (HK) and its cognate DosR response regulator (RR) (24, 26, 29). The DosT HK, which shares high sequence similarity to DosS over the length of their primary structures, was also found to cross talk with DosR (26, 30). The N-terminal domains of DosS and DosT contain two tandem GAF domains (GAF-A and GAF-B from their N termini), and the three-dimensional structure of the GAF-A and GAF-B domains was determined (5, 25). A *b*-type heme is embedded in the GAF-A domain, composed of one five-stranded antiparallel β-sheet and four α-helices (5, 14, 25, 32). The heme is positioned nearly perpendicular to the β-sheet, and H149 and H147 of the polypeptides serve as the proximal axial ligands for DosS and DosT, respectively (5, 25). The ligand-binding state at the distal axial position of heme and the redox state of the heme iron modulate the autokinase activity of DosS and DosT. The O_2-bound (oxyferrous) and ferric forms of the HKs are inactive, whereas the unliganded ferrous (deoxyferrous) form as well as NO- and CO-bound forms are active (17, 36). The heme iron of DosT is stable against autooxidation of Fe^{2+} to Fe^{3+} in the presence of O_2, indicating that its conversion between deoxyferrous and oxyferrous forms is the mechanism by which DosT recognizes O_2 (17). However, the autooxidation property of oxyferrous DosS remains controversial. Kumar et al. (17) and Cho et al. (5) reported that DosS undergoes autooxidation on exposure to O_2, while other research groups demonstrated that the oxyferrous form of DosS is stable against autooxidation (13, 14, 36). Recently, different roles of DosS and DosT in O_2 sensing by *M. tuberculosis* were suggested. DosT plays a more important role in the early phase of hypoxic conditions than DosS when the growth of *M. tuberculosis* is transferred from aerobic to hypoxic conditions (11).

Mycobacterium smegmatis possesses a single DevS HK that phosphorylates the DevR RR (20). The DevSR two-component system is also implemented in hypoxic adaptation of this bacterium (20). Like DosT of *M. tuberculosis*, the autokinase activity of *M. smegmatis* DevS was shown to be controlled by the ligand-binding state of its heme (18). Regarding the autooxidation property, DevS of *M. smegmatis* was suggested to be similar to DosT rather than DosS; i.e., the heme iron in DevS is resistant to autooxidation from an oxyferrous to a ferric state in the presence of O_2 (18).

In this paper we report several lines of evidence for the functional difference between DosS and DosT in the hypoxic adaptation of mycobacteria and discuss the implications of these findings.

MATERIALS AND METHODS

Bacterial strains, plasmids, and culture conditions. The bacterial strains and plasmids used in this study are listed in Table 1. *M. smegmatis* strains were grown in Middlebrook 7H9 medium (Difco, Sparks, MD) supplemented with 0.2% (wt/vol) glucose as a carbon source and 0.02% (vol/vol) Tween 80 as an anticlumping agent at 37°C. *M. smegmatis* strains were grown either aerobically in a

* Corresponding author. Mailing address: Department of Microbiology, Pusan National University, Busan 609-735, Republic of Korea. Phone: 82-51-510-2593. Fax: 82-51-514-1778. E-mail: joh@pusan.ac.kr.

▽ Published ahead of print on 30 July 2010.

TABLE 1. Bacterial strains and plasmids used in this study

Strain or plasmid	Relevant phenotype or genotype	Reference or source
Strains		
E. coli		
DH5α	(ϕ80d*lacZ*ΔM15) Δ*lacU169 recZ1 endA1 hsdR17 supE44 thi-1 gyrA96 relA1*	15
BL21(DE3)	F^- *ompT hsdS*$_B$ (r_B^- m_B^-) *dcm gal* λ(DE3)	Promega
M. smegmatis		
mc^{2}155	High-transformation-efficiency mutant of *M. smegmatis* ATCC 607	35
mc^{2}155 Δ*devS*	*devS* deletion mutant derived from *M. smegmatis* mc^{2}155	This study
Plasmids		
pBluescript II KS+	Amp^r; *lacPOZ′*	This study
pKO	Hyg^r; *sacB*, suicide vector	34
pUC19	Amp^r; *lacPOZ′*	42
pHIS-parallel	Amp^r; T7 promoter, rTEV protease cleavage site, and containing 6 His codons after translation start codon	33
pNBV1	Hyg^r; 5.8-kb plasmid derived from p16R1	12
pBSDevS	pBluescript II KS+::1.9-kb BamHI-XhoI fragment containing *devS*	This study
pBSDevS2	pBluescript II KS+::1.8-kb BamHI-XhoI fragment containing Δ*devS*	This study
pBSDosS	pBluescript II KS+::1.9-kb BamHI-XhoI fragment from pHis-DosS	This study
pBSDosT	pBluescript II KS+::1.9-kb BamHI-XhoI fragment from pHis-DosT	This study
pBSDosST	pBluescript II KS+::2.0-kb HindIII-XbaI fragment containing *dosST*	This study
pBSDosTA	pBluescript II KS+::2.0-kb HindIII-XbaI fragment containing *dosTS*	This study
pKOΔdevS	pKO::1.8-kb BamHI-XhoI fragment containing Δ*devS*	This study
pUCSHis	pUC19::1.7-kb BamHI fragment containing *devS* with 6 His codons before its stop codon; *devS* is colinear to *lacZ*	This study
pHis-DosS	pHis-parallel1::1.7-kb NcoI-HindIII fragment containing *dosS* of *M. tuberculosis*	B. S. Kang, unpublished data
pHis-DosT	pHis-parallel1::1.7-kb NcoI-HindIII fragment containing *dosT* of *M. tuberculosis*	B. S. Kang, unpublished data
pNBV1SHis	pNBV1::1.7-kb BamHI fragment containing *devS* with 6 His codons before its stop codon; *devS* is colinear to *lacZ*	This study
pNBV1DosT	pNBV1::1.8-kp HindIII-XbaI fragment containing *dosT* of *M. tuberculosis* with 6 His codons before its start codon	This study
pNBV1DosS	pNBV1::1.9-kp HindIII-XbaI fragment containing *dosS* of *M. tuberculosis* with 6 His codons before its start codon	This study
pNBV1DosST	pNBV1::2.0-kb HindIII-XbaI fragment containing *dosST*	This study
pNBV1DosTS	pNBV1::2.0-kb HindIII-XbaI fragment containing *dosTS*	This study
pNBV1DosSE87G	pNBV1DosS in which the codon for E87 is replaced with GGG	This study
pNBV1DosSH89R	pNBV1DosS in which the codon for H89 is replaced with CGC	This study
pNBV1DosSD90G	pNBV1DosS in which the codon for D90 is replaced with CCG	This study
pNBV1DosSH97E	pNBV1DosS in which the codon for H97 is replaced with GAA	This study
pNBV1DosSV108R	pNBV1DosS in which the codon for V108 is replaced with CGG	This study
pNBV1DosSV118R	pNBV1DosS in which the codon for V118 is replaced with CGA	This study
pNBV1DosST169N	pNBV1DosS in which the codon for T169 is replaced with AAT	This study

250-ml Erlenmeyer flask filled with 100 ml of 7H9-glucose medium on a gyratory shaker (200 rpm) to an optical density at 600 nm (OD_{600}) of 0.5 or under hypoxic conditions in a 250-ml flask filled with 150 ml of 7H9-glucose medium (the ratio of headspace volume to culture volume was 0.87) and tightly sealed with a rubber stopper on a gyratory shaker (200 rpm) for 20 or 50 h following inoculation of the medium with aerobically grown preculture to an OD_{600} of 0.05, which allowed a gradual depletion of O_2 from the growth medium. When methylene blue (1.5 μg/ml) was added to the hypoxic culture medium as an oxygen indicator, the complete decolorization of methylene blue was observed to occur at between 33 and 34 h after the cultivation was initiated. When required, hygromycin (50 μg/ml) was added to the growth medium. *Escherichia coli* strains were grown in Luria-Bertani (LB) medium at 37 or 30°C. When required, hygromycin (200 μg/ml) or ampicillin (100 μg/ml) was added to the growth medium for *E. coli*.

DNA manipulation and electroporation. Standard protocols or manufacturer's instructions were followed for recombinant DNA manipulations (31). The introduction of plasmids into *M. smegmatis* strains was carried out by electroporation as described elsewhere (35).

Construction of a *devS* mutant. To construct a *devS* mutant, a 1,847-bp fragment containing the *devS* gene was amplified from chromosomal DNA of *M. smegmatis* by PCR using *Pfu* DNA polymerase and the primer pair SF-BamHI (5′-GCCGGGATCCGACGAAAGTG-3′) and DevS-M-XhoI (5′-AAGCCTCG AGGAACTCGACCG-3′). The PCR product was restricted with BamHI and XhoI and cloned into pBluescript II KS+ to give the plasmid pBSDevS. A 69-bp PstI fragment was deleted by restriction of pBSDevS with PstI and self-ligation of the vector part, resulting in the plasmid pBSDevS2. Finally, a 1,778-bp BamHI-XhoI fragment from pBSDevS2 was cloned into the suicide vector pKO, yielding the plasmid pKOΔdevS. The resulting plasmid, pKOΔdevS, was introduced into *M. smegmatis* mc^{2}155 by electroporation to generate a Δ*devS* mutant. Heterogenotes of *M. smegmatis*, generated by a single recombination event, were selected for their hygromycin resistance on 7H9-glucose agar plates. Isogenic homogenotes were obtained from the heterogenotes after a second recombination by selecting for sucrose resistance on 7H9-glucose agar plates containing 10% (wt/vol) sucrose. The allelic exchange was verified by PCR.

Construction of plasmids used for complementation. A 1,864-bp HindIII-XbaI fragment containing *dosS* of *M. tuberculosis* was obtained by restriction of pHis-DosS with HindIII and XbaI and cloned into pBluescript II KS+ restricted with the same enzymes, giving the plasmid pBSDosS. The HindIII-XbaI fragment from pBSDosS was cloned into the shuttle vector pNBV1 to yield pNBV1DosS.

A 1,800-bp HindIII-XbaI fragment containing *dosT* of *M. tuberculosis* from pHis-DosT was digested with HindIII and XbaI and cloned into pBluescript II KS+, yielding the plasmid pBSDosT. The plasmid pNBV1DosT was constructed from pBSDosT in the same way as pNBV1DosS.

To construct pNBV1SHis, a 1,715-bp fragment containing the *devS* gene with a tail of six histidine codons before its stop codon was amplified from pBSDevS by PCR using forward primer SF-BamHI (5′-GCCGGGATCCGACGAAAGT G-3′) and reverse primer SHis (5′-ATGCGGATCCTCAGTGGTGGTGATGG

TGGTGGTCGGGGAGCGGCGCGGT-3′). The PCR product was restricted with BamHI and cloned into pUC19 to give the plasmid pUCSHis. Finally, a 1,715-bp BamHI fragment was cloned into pNBV1 restricted with BamHI, resulting in the plasmid pNBV1SHis.

Construction of chimeric histidine kinases. The chimeric DosST histidine kinase consists of the GAF-A domain of DosS (M1 to A218) and the GAF-B and kinase domains of DosT (T217 to R573). The chimeric DosTS consists of the GAF-A domain of DosT (M1 to A216) and the GAF-B and kinase domains of DosS (T219 to Q578). To construct the chimeric gene for DosST, an 840-bp DNA fragment encoding the GAF-A domain of DosS was generated by PCR using pBSDosS as the template and the primer pair T7 (5′-CGACTCACTATA GGGCG-3′) and GafAS-R (5′-GTTCCGATGTCGCGGGTGGCCTCGATCC ACGACT-3′). A 1,172-bp DNA fragment encoding the GAF-B and kinase domains of DosT was obtained by PCR using pBSDosT as the template and the primers GafBT-F (5′-AGTCGTGGATCGAGGCCACCCGCGACATCGGAA C-3′) and T3 (5′-TAACCCTCACTAAAGGG-3′). In the secondary PCR, the DNA fragment encoding the chimeric DosST was then obtained by using both the primary PCR products as the templates and the T3 and T7 primers. A 2,012-bp PCR product was digested with HindIII and XbaI and ligated to pBluscript II KS+ digested with the same restriction enzymes, yielding pBSDosST. The recombinant gene on pBSDosST was verified by DNA sequencing. The 2.0-kb HindIII-XbaI fragment from pBSDosST was cloned into the pNBV1 vector, giving the plasmid pNBV1DosST. The same strategy was used for the construction of pNBV1DosTS containing the chimeric *dosTS* gene. An 834-bp DNA fragment encoding the GAF-A domain of DosT was amplified by PCR using pBSDosT as the template and the primers T7 and GafAT-R (5′-G TGGCGATGTCACGGGTTGCCTCGATCCACGCTT-3′). A 1,163-bp DNA fragment encoding the GAF-B and kinase domains of DosS was generated by PCR using pBSDosS as the template and the primers GafBS-F (5′-AAGCGTG GATCGAGGCAACCCGTGACATCGCCAC-3′) and T3. The secondary PCR was performed with the primary PCR products and the T3 and T7 primers. The remaining procedure for the construction of pNBV1DosTS was the same as that described for the construction of pNBV1DosST.

Site-directed mutagenesis. To introduce point mutations E87G, H89R, D90G, H97E, V108R, V118R, and T169N into DosS, mutagenesis was carried out using the QuikChange site-directed mutagenesis procedure (Stratagene, La Jolla, CA). The plasmid pBSDosS was used as the template in PCRs using *Pfu* DNA polymerase. Synthetic oligonucleotides 33 to 34 bases long containing a mutated codon in the middle of their sequences were employed to mutagenize the original codons. Following the verification of mutations by DNA sequencing, 1.9-kb HindIII-XbaI fragments were cloned into pNBV1.

RT-PCR and qRT-PCR. RNA isolation from *M. smegmatis* strains was carried out as described elsewhere (22) after disrupting *M. smegmatis* cells using TRIzol (Invitrogen, Carlsbad, CA) and a Fastprep 120 beadbeater (Thermo, Milford, MA). cDNA was synthesized by RT-&GO Mastermix reverse transcriptase (MPbio, Eschwege, Germany) according to the manufacturer's instruction. Synthesis of cDNA was performed using 1 μg of the isolated total RNA as the template as well as primers RT-16sr(−) (5′-ACAACGCTCGGACCCTAC-3′) and Rihsp(−) (5′-CGCCCGTTGGTCTCCTTCTTC-3′) for the 16S rRNA and *hspX* genes, respectively. For reverse transcription-PCR (RT-PCR), primers RT-16sr(+) (5′-CTGGGACTGAGATACGGC-3′) and RT-16sr(−) for the 16S rRNA gene as well as primers Rihsp(+) (5′-GGGTCT GCCGTCGTGGGCCTC-3′) and Rihsp(−) for the *hspX* gene were used. RT-PCR was carried out in a 20-μl mixture containing 1 μl of the synthesized cDNA, 15 pmol each of the primers, 0.1 mM deoxynucleoside triphosphates (dNTPs), and 0.5 unit of *Taq* DNA polymerase. Thermal cycling began with an initial step at 94°C for 5 min, followed by 15 cycles of 94°C for 1 min, 52°C for 30 s, and 72°C for 14 s, and ended with a step at 72°C for 5 min. For quantitative real-time PCR (qRT-PCR), the same primer sets as described for RT-PCR were employed. PCR was performed using DyNamo SYBR green qPCR kit (Bio-Rad, Hercules, CA). qRT-PCR was performed in a 20-μl mixture containing 10 ng of the template cDNA, 15 pmol of each of the primers, 10 μl of iQ SYBR green Supermix (Bio-Rad), and 7 μl of distilled H_2O. Thermal cycling began with and initial step at 94°C for 5 min, followed by 40 cycles of 94°C for 1 min, 52°C for 30 s, and 72°C for 14 s. qRT-PCR data were analyzed with MJ Opiconmonitor analysis software version 3.1 (Bio-Rad).

RESULTS

Phylogenetic analysis of the GAF-A domains of mycobacterial DevS (DosS, DosT) homologs. *M. smegmatis* has a single DevS HK, unlike *M. tuberculosis*, which has both DosS and DosT HKs (20). The autooxidation property and O_2-sensing mechanism of *M. smegmatis* DevS were demonstrated to be more similar to those of DosT than those of DosS (17, 18). Since the GAF-A domains of DosS and DosT are involved in heme binding (5, 14, 25, 32), we assumed that the different O_2-sensing mechanism of the mycobacterial DevS homologs might be attributable to the difference in their GAF-A domains. The phylogenetic analysis of the GAF-A domains of the mycobacterial DevS homologs revealed that the primary structure of the GAF-A domain of *M. smegmatis* DevS is more closely related to that of DosT than DosS (Fig. 1). In the phylogenetic tree, the DosS homologs are present in *M. tuberculosis* and *Mycobacterium bovis* as well as *Mycobacterium kansasii*, *Mycobacterium marinum*, and *Mycobacterium ulcerans*. The DosT homologs were found in *M. tuberculosis*, *M. bovis*, *M. smegmatis*, *Mycobacterium gilvum*, and *Mycobacterium vanbaalenii*. *Mycobacterium avium*, *M. kansasii*, and *M. marinum* contain the DevS homologs, which form a phylogenetically distinct branch from both DosS and DosT of *M. tuberculosis*.

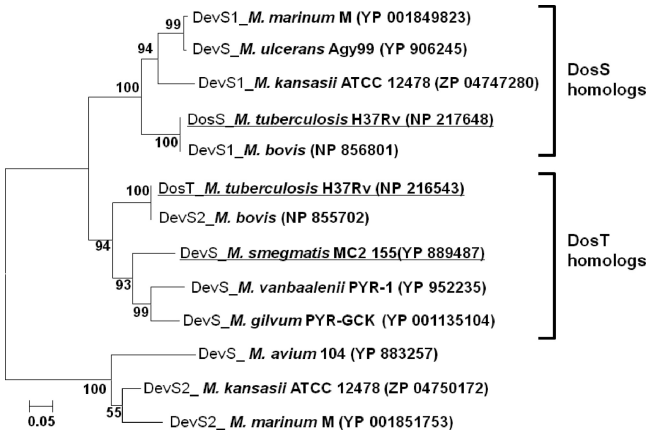

FIG. 1. Phylogenetic analysis of the GAF-A domains of mycobacterial DevS (DosS, DosT) homologs. Phylogenetic analysis was performed using the neighbor-joining method. Bootstrap values, expressed as percentages of 1,000 replications, are given at the nodes. The scale bar indicates 0.05 nucleotide substitution per nucleotide position. The strains relevant to this study are underlined. The GenBank accession numbers of the amino acid sequences are given in parentheses.

DosT, but not DosS, can functionally substitute for DevS of *M. smegmatis*. On the basis of the phylogenetic analysis and the reported autooxidation properties of DevS, DosS, and DosT, we presumed that DosT of *M. tuberculosis* could functionally substitute for DevS of *M. smegmatis*. To examine this, complementation analysis using a *devS* deletion mutant (Δ*devS*) of *M. smegmatis* was performed. The reporter gene used in the complementation test was the *hspX* gene, whose expression was known to be strongly induced under hypoxic conditions by the DevSR two-component system (3, 7, 9, 10, 21, 34, 39, 43). To examine whether the introduction of the *devS*, *dosS*, and *dosT* genes into the Δ*devS* mutant strain of *M. smegmatis* led to the complementation of a *devS* mutant phenotype, *hspX* gene expression was determined by RT-PCR (Fig. 2). The Δ*devS* mutant strain of *M. smegmatis* with the empty pNBV1 vector was used as a negative control. As expected, expression of *hspX* in the Δ*devS* mutant strain with pNBV1 was not induced under

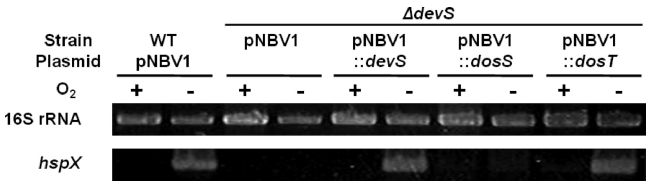

FIG. 2. Expression of *hspX* in *M. smegmatis* strains grown under aerobic or hypoxic conditions. *M. smegmatis* strains with the expression plasmid pNBV1SHis (pNBV1::*devS*), pNBV1DosS (pNBV1::*dosS*), or pNBV1DosT (pNBV1::*dosT*) were used for complementation analysis. The complementation test was performed by determining the expression levels of *hspX* in *M. smegmatis* strains grown under either aerobic (O_2+) or hypoxic (O_2-) conditions for 20 h by means of RT-PCR. As controls, the wild-type (WT) and Δ*devS* mutant strains of *M. smegmatis* containing the empty vector pNBV1 were included in the test. RT-PCR for the 16S rRNA gene was performed to ensure that the same amounts of total RNA were employed for RT-PCR.

hypoxic conditions, whereas the introduction of *devS* into the mutant led to the restoration of hypoxic induction of *hspX* to the level observed in the wild-type strain of *M. smegmatis* with pNBV1. When *dosT* of *M. tuberculosis* was introduced into the Δ*devS* mutant strain, *hspX* gene expression was restored under hypoxic conditions. In contrast, the introduction of *dosS* did not result in the hypoxic induction of *hspX* in the Δ*devS* mutant strain. Since both *dosS* and *dosT* cloned into pNBV1 have the same promoter and control sequences upstream of their start codons, this result indicates that DosT, not DosS, is able to functionally substitute for DevS of *M. smegmatis* and that the functional difference between DosS and DosT is not the consequence of their different expression patterns.

The different roles of DosS and DosT in the adaptation of *M. smegmatis* to hypoxic conditions. Recently it has been suggested by examining the survival rates of *dosS* and *dosT* mutant strains of *M. tuberculosis* under hypoxic and anaerobic conditions that DosT plays a more important role in the hypoxic adaptation of this bacterium in the early phase of the transition from aerobic to hypoxic conditions than DosS and that DosS plays a predominant role in the hypoxic adaptation at the later phase (11). This suggestion led us to examine the possibility that the duration of hypoxic conditions in the experiment described in Fig. 2 (20 h) might be too short to activate the kinase activity of DosS. As shown in Fig. 3, expression of *hspX* was not induced in the Δ*devS* mutant strain with DosS which was grown under hypoxic conditions for 20 h. However, when the Δ*devS* mutant with DosS was grown under hypoxic conditions for 50 h, *hspX* expression was slightly induced. In contrast, expression of *hspX* was strongly induced in the Δ*devS* mutant with DosT grown under hypoxic conditions for 20 h and was significantly reduced, to the level observed in the Δ*devS* mutant with DosS, when the mutant strain was grown under hypoxic conditions for 50 h. The Δ*devS* mutant with DevS showed the same expression pattern of *hspX* as the Δ*devS* mutant with DosT, which is in good agreement with the complementation results. As expected, the *hspX* gene was not induced in the Δ*devS* mutant harboring the empty vector pNBV1 under both hypoxic conditions (20 and 50 h). These results imply the following: (i) DosT appears to respond to a decrease in oxygen tension more sensitively than DosS; (ii) the DosR regulon is induced mainly during the early phase of transition from aerobic to hypoxic

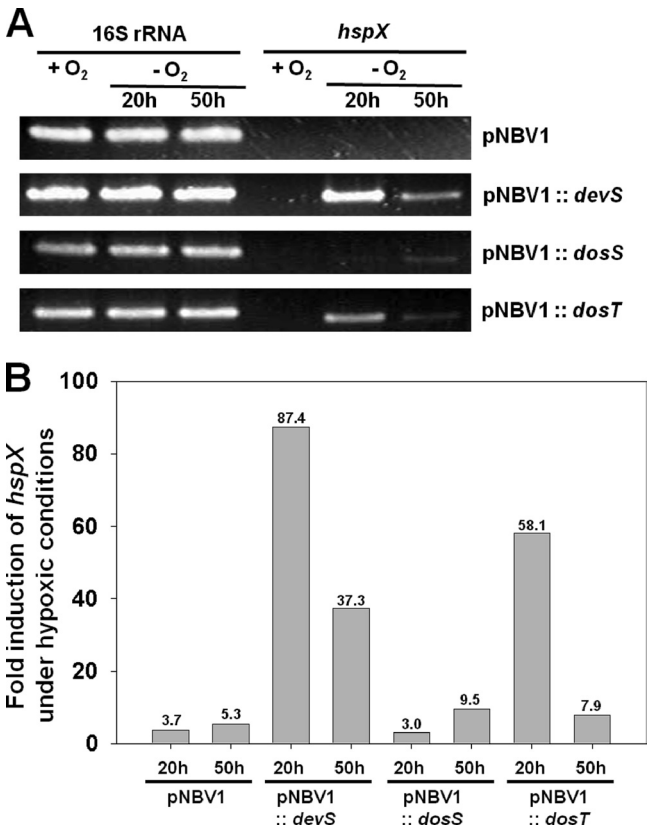

FIG. 3. Different responsiveness of DosS and DosT to hypoxia. The expression levels of *hspX* in the Δ*devS* mutant strains of *M. smegmatis* containing the expression plasmid pNBV1, pNBV1SHis (pNBV1::*devS*), pNBV1DosS (pNBV1::*dosS*), or pNBV1DosT (pNBV1::*dosT*) were determined by means of RT-PCR (A) and qRT-PCR (B). *M. smegmatis* strains were grown under either aerobic ($+O_2$) or hypoxic ($-O_2$) conditions for 20 and 50 h. As controls, the Δ*devS* mutant strains of *M. smegmatis* containing either the empty vector pNBV1 or pNBV1SHis were included in the experiment. The levels of mRNA specific for *hspX* were determined by qRT-PCR and normalized to those of 16S rRNA. Fold induction of *hspX* expression indicates the level of *hspX* mRNA in hypoxic culture relative to that in aerobic culture.

conditions; and (iii) when oxygen tensions in the growth medium are gradually decreased to reach very low oxygen or anaerobic conditions, the expression of the DosR regulon is significantly reduced. This is consistent with the results of Honarker et al. (11).

The discrepancy in the complementation abilities of DosS and DosT is attributable to the difference in the primary structures of their GAF-A domains. The results from phylogenetic analysis and complementation tests suggest that the difference between DosS and DosT regarding the complementation of the Δ*devS* mutant strain of *M. smegmatis* might be caused by a structural difference in their GAF-A domains, which serve as the heme-binding domain. To examine this possibility, we constructed two kinds of chimeric histidine kinases, DosST and DosTS. DosST is a chimeric construct in which the GAF-A domain of DosT is replaced with that of DosS. Likewise, DosTS has the GAF-A domain of DosT instead of that of DosS (Fig. 4A). The genes encoding these constructs were

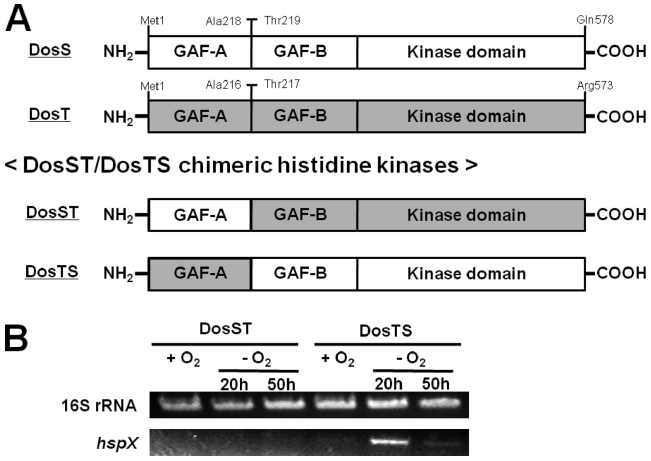

FIG. 4. Schematic diagram depicting the chimeric DosST and DosTS HKs (A) and complementation analysis using the Δ*devS* mutant strain of *M. smegmatis* with DosST and DosTS (B). The chimeric DosST HK consists of the GAF-A domain of DosS (M1 to A218) and the GAF-B and kinase domains of DosT (T217 to R573). The chimeric DosTS HK consists of the GAF-A domain of DosT (M1 to A216) and the GAF-B and kinase domains of DosS (T219 to Q578). The plasmids pNBV1DosST and pNBV1DosTS, containing the genes encoding DosST and DosTS, respectively, were introduced into the Δ*devS* mutant strain of *M. smegmatis*, and the complementation test was performed by determining the expression levels of *hspX* in *M. smegmatis* strains grown under either aerobic ($+O_2$) or hypoxic ($-O_2$) conditions for 20 and 50 h by means of RT-PCR. RT-PCR for the 16S rRNA gene was performed to ensure that the same amounts of total RNA were employed in RT-PCR.

cloned into pNBV1, and the resulting plasmids (pNBV1DosST and pNBV1DosTS) were introduced into the Δ*devS* mutant of *M. smegmatis*.

The Δ*devS* mutant strains of *M. smegmatis* harboring pNBV1DosST or pNBV1DosTS were grown either aerobically or under hypoxic conditions for 20 and 50 h, and the expression of *hspX* was determined by RT-PCR. As shown in Fig. 4B, the Δ*devS* mutant strain with DosTS showed the same *hspX* expression pattern as the Δ*devS* mutant with DosT. Expression of *hspX* was strongly induced in the Δ*devS* mutant strain with DosTS grown under hypoxic conditions for 20 h and significantly decreased when the mutant was grown under hypoxic conditions for 50 h. In contrast, DosST did not induce *hspX* expression in the Δ*devS* mutant grown under hypoxic conditions. This finding strongly indicates that the discrepancy in the complementation abilities of DosS and DosT results not from the difference in their GAF-B and kinase domains but from that in their GAF-A domains.

As an initial attempt to identify the amino acid residues within the GAF-A domain which confer the functional difference between DosS and DosT, multiple alignment was performed on the GAF-A domains of DevS homologs belonging to the DosS and DosT subclades in the phylogenetic tree (Fig. 5). The multiple-alignment analysis of the GAF-A domains showed that seven amino acids were conserved differentially between the DosS and DosT homologs, even though the majority of the amino acids of the GAF-A domains were well conserved, implying that those amino acid residues showing specific variations between DosS and DosT might be responsible for the different functionality of DosS and DosT.

To assess the whether or not the seven differentially conserved amino acids are indeed related to the different functionality of DosS and DosT, the amino acids of DosS were replaced with those corresponding to DosT using site-directed mutagenesis. The mutated genes were cloned into pNBV1 and introduced into the Δ*devS* mutant of *M. smegmatis*. We reasoned that the corresponding amino acid might be important in DosS- or DosT-specific function if a mutant form of DosS complements the Δ*devS* mutant of *M. smegmatis* in terms of hypoxic induction of *hspX*. The RT-PCR result presented in Fig. 6A shows that the E87G, D90G, H97E, L118R, and T169N mutant forms of DosS complemented the *devS* mutant phenotype, whereas the H89R and V108R mutant forms did not. The *hspX* gene expression levels were also determined

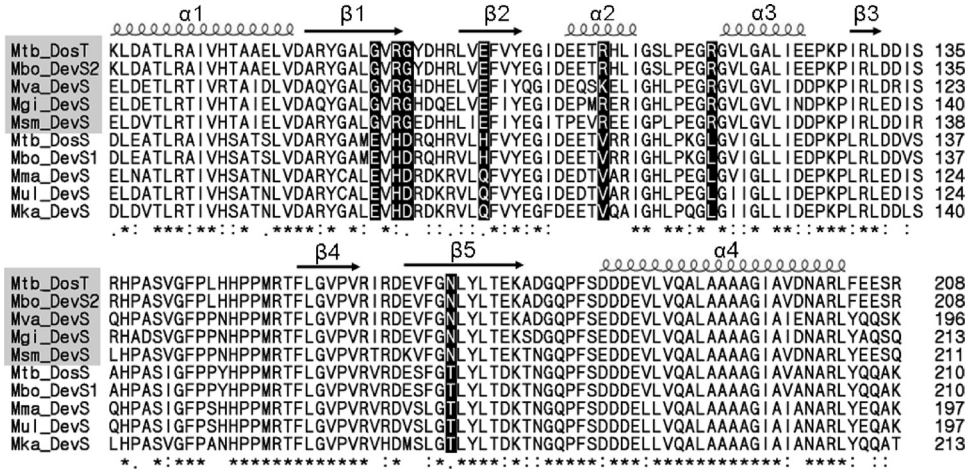

FIG. 5. Multiple alignment of the GAF-A domains of mycobacterial DosS and DosT homologs. Multiple alignment was generated by using ClustalW. Identical and conservatively substituted residues are indicated by asterisks and colons, respectively. The arrows and coils indicate the positions of α-helices and β-strands, respectively. The amino acid residues conserved differentially between the DosS and DosT subclades are highlighted in black. The DosT homologs are shaded by the gray boxes. Abbreviations: Mbo, *M. bovis*; Mgi, *M. gilvum*; Mka, *M. kasasii*; Mma, *M. marinum*; Msm, *M. smegmatis*; Mtb, *M. tuberculosis*; Mul, *M. ulcerans*; Mva, *M. vanbaalenii*.

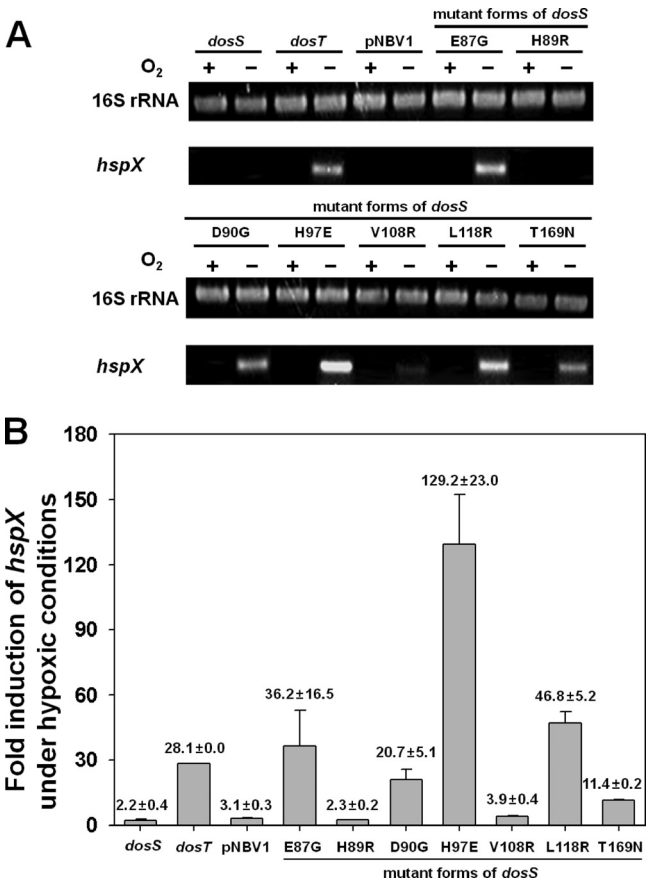

FIG. 6. Effect of E87G, H89R, D90G, H97E, V108R, L118R, and T169N mutations on the sensory function of DosS *in vivo*. Complementation tests were performed by determining the expression levels of *hspX* in *M. smegmatis* strains grown under either aerobic (O_2+) or hypoxic (O_2−) conditions for 20 h by means of RT-PCR (A) and qRT-PCR (B). The Δ*devS* mutant strains were complemented with the wild-type *dosS* and *dosT* as well as the E87G, H89R, D90G, H97E, V108R, L118R, and T169N mutant forms of *dosS*. As a control, the Δ*devS* mutant strain of *M. smegmatis* containing the empty vector pNBV1 was included in the experiment. The strains were grown under either aerobic (O_2+) or hypoxic (O_2−) conditions for 20 h. The levels of mRNA specific for *hspX* were determined by qRT-PCR and normalized to those of 16S rRNA. Fold induction of *hspX* expression indicates the level of *hspX* mRNA of hypoxic culture relative to that of aerobic culture. All values provided are the averages of results of two independent determinations. Error bars indicate standard deviations.

quantitatively by means of qRT-PCR. As shown in Fig. 6B, the extent of *hspX* gene expression observed in RT-PCR correlated well with that determined by qRT-PCR assay. The levels of *hspX* induction in the Δ*devS* mutant strains with the E87G, H97E, and L118R mutant forms of DosS were comparable to or greater than that observed for the Δ*devS* mutant harboring DosT. Especially, the level of *hspX* expression was increased approximately 4-fold in the Δ*devS* mutant with H97E DosS compared with the Δ*devS* mutant with DosT. Taken together, these results indicate that just one substitution of E87, D90, H97, L118, or T169 of DosS with the corresponding residue of DosT is sufficient to convert the functionality of DosS to that of DosT.

DISCUSSION

The different roles of DosS and DosT in the hypoxic response of mycobacteria. The DosR (DevR) regulon was suggested to play a significant role in survival of mycobacteria under respiratory stress conditions such as hypoxic, NO, and CO conditions where the growth of the bacteria is halted by the inhibition of aerobic respiration (3, 11, 19, 23, 27, 34, 38). Several studies showed that induction of the DosR regulon occurs in the early phase of progressive hypoxia *in vitro*, and such an initial hypoxic response appears to prime mycobacteria for subsequent adaptation to and survival in extended and more unfavorable anaerobiosis (27, 40, 41). The DosR regulon is regulated by the DosR RR, whose activity is controlled by two homologous HKs, DosS and DosT. In *M. tuberculosis*, the *dosS* gene forms the same transcriptional unit with *dosR* and its expression is induced under hypoxic conditions, whereas the *dosT* gene is constitutively expressed under both aerobic and hypoxic conditions (11, 30). This different expression pattern gives DosT an advantage over DosS in the initial hypoxic adaptation of *M. tuberculosis* during the transition from aerobic to hypoxic conditions (11).

In this study, we found by complementation tests that DosT strongly induced the expression of *hspX* in 20-h hypoxic culture of *M. smegmatis*, as was the case for DevS of *M. smegmatis*. In contrast, DosS did not lead to the induction of *hspX* in 20-h hypoxic culture of *M. smegmatis*. As the duration of hypoxic stress increased (50 h of hypoxic conditions), the expression of *hspX* by DosT was significantly reduced. Interestingly, DosS induced *hspX* expression at a higher level under 50 h of hypoxic conditions than under 20 h of hypoxic conditions, indicating that DosS has a lower threshold value of oxygen tension to activate the transcription of the DosR regulon than DosT and that DosT and DosS are inefficient in phosphorylation of DosR under very low oxygen or anaerobic conditions. We can rule out the possibility that the less sensitive response of DosS to hypoxia than of DosT results from the difference in their expression patterns, because *dosS* and *dosT* cloned into the expression vector have the same promoter and control regions. Our finding suggests that the presence of both DosS and DosT paralogs in *M. tuberculosis* is not a functional redundancy but that they play distinct roles in sensing changing oxygen tension. When *M. tuberculosis* is gradually transited from aerobic to anaerobic conditions, DosT appears to first respond to a decline in oxygen tension, resulting in the induction of the DosR regulon, including *dosS*. As the synthesis of DosS is induced and oxygen tension is further decreased, DosS plays a predominant role in the later phase of the hypoxic adaptation of *M. tuberculosis*. This finding is in good agreement with the results obtained by Honaker et al. (11).

Our complementation tests also showed that DosT, but not DosS, is a functional substitute for DevS of *M. smegmatis*. What is a property that DosT and DevS share and DosS does not have? Although it is controversial, both DevS and DosT are resistant to autooxidation of the heme iron in the presence of oxygen, whereas a deoxyferrous form of DosS is quickly autooxidized to a ferric form on exposure to oxygen (5, 17, 18). Since the autooxidation property of a heme is determined by the microenvironment surrounding the heme, the difference in autooxidation properties of DosS and DosT is likely attribut-

able to the structural difference in their GAF-A domains. Complementation analysis using the domain-swapped DosST and DosTS HKs clearly demonstrated that it is the GAF-A domain that determines the different responsiveness of DosS and DosT to hypoxia, which might result from their different autooxidation properties. In good agreement with the complementation results, phylogenetic analysis of the GAF-A domains of mycobacterial DevS (DosS and DosT) homologs revealed that DosT of *M. tuberculosis* and DevS of *M. smegmatis* belong to the same subclade, which is separated from the DosS subclade, indicating that DevS is more closely related to DosT than DosS. DevS of *M. avium*, DevS2 of *M. kansasii*, and DevS2 of *M. marinum* form a separate subclade from DosS and DosT (Fig. 1). Based on our finding that E87G and L118R substitutions of DosS lead to the conversion of DosS to DosT in terms of the initial hypoxic induction of *hspX* (Fig. 6), the DevS homologs in the third subclade are assumed to be of the DosT type due to the presence of alanine and lysine at positions E87 and L118, respectively.

It is noteworthy that the nonpathogenic mycobacteria such as *M. smegmatis*, *M. gilvum*, and *M. vanbaalenii* have a single DosT homolog. In contrast, most pathogenic mycobacteria contain two DevS homologs, comprising one DosS homolog and either a DosT homolog or a DevS homolog belonging to the third subclade. This finding implies that DosS homologs likely give the pathogenic mycobacteria a better chance to survive and develop pathogenicity within their hosts. In accordance with this, Converse et al. reported that the survival rate and virulence of *M. tuberculosis* in the mouse and guinea pig models are diminished when *dosS* expression is disrupted (6).

The micromilieu of the distal ligand-binding pocket might determine the different responsiveness of DosS and DosT to hypoxic conditions. The difference in the sensitivity of DosS and DosT to respond to changes in oxygen tension is likely due to the difference in their oxygen-sensing mechanism. In the case of DosT, a decrease in oxygen tension is sensed through simple changes in the ligand-binding state of the heme, i.e., from an oxyferrous to a deoxyferrous form, while DosS perceives a reduction in oxygen tension through the conversion of the redox state of its heme from a ferric to a ferrous form, which probably requires a reductase and reductant system(s) as well as sufficiently low oxygen tension (13, 17). According to the model for autooxidation of myoglobin proposed by Brantley et al. (4), the binding of O_2 to the distal coordination position of the ferrous heme and the subsequent protonation of O_2 lead to spontaneous dissociation of the neutral superoxide radical with concomitant oxidation of the heme iron from Fe^{2+} to Fe^{3+}. A water molecule can then serve as a distal ligand of the heme in place of O_2. Therefore, the autooxidation of the heme requires the presence of oxygen and water as well as a proton donor.

The rate of autooxidation of the heme iron is affected by the microenvironment governed by amino acid residues lining the heme-binding pocket (1, 2, 4). The steric hindrance to O_2 bound to the heme by the side chains of amino acid residues in the distal ligand-binding pocket promotes displacement of both O_2 and its protonated form, which results in an enhancement of the autooxidation rate (2, 4). The polarity and size of the distal ligand-binding pocket are also known to influence the rate of autooxidation of the heme (1, 2, 4). Multiple-alignment analysis of the GAF-A domains of mycobacterial DosS (DosT) homologs and subsequent site-directed mutagenesis revealed that just one substitution of E87, D90, H97, L118, or T169 of DosS with the corresponding residue of DosT is enough to convert the functionality of DosS to that of DosT. Although experimental validation is required, this finding allowed us to hypothesize that a single point mutation in DosS (E87G, D90G, H97E, L118R, and T169N) leads to the inhibition of autooxidation of the heme iron of DosS. Interestingly, all the amino acid residues of DosS (E87, D90, H97, L118, and T169) identified to be responsible for functional conversion from DosS to DosT are located at the β1, β2, and β5 strands as well as at the β1-β2 and α2-α3 connecting loops that form the ligand-binding pocket on the distal side of the heme (5, 25). The failure of V108R and H89R mutations in the functional conversion can be explained by the facts that V108 of DosS occurs at the α2 helix located on the proximal side of the heme and that H89 is conservatively substituted by arginine. This result confirms that the environment in the ligand-binding pocket on the distal side of the heme is important in determining the different functionalities of DosS and DosT. Recently, the three-dimensional structure of the DosS GAF-A domain was determined, and a hydrogen-bonding network consisting of H89, E87, and Y171 was suggested (5). The network was suggested to serve as a pathway for electron transport for the reduction of Fe^{3+} to Fe^{2+} (5). It is also possible that a proton is transferred via this hydrogen-bonding pathway to the O_2 molecule bound to heme to facilitate the formation of the neutral superoxide radical, which in turn leads to autooxidation of the heme iron. Since the hydrogen-bonding network is disrupted in E87G DosS, this mutant form of DosS possibly possesses a DosT-like property in terms of the autooxidation rate.

In conclusion, we demonstrated *in vivo* that DosS and DosT of *M. tuberculosis* play differential roles in hypoxic adaptation. DosT responds to a decrease in oxygen tension more sensitively and strongly than DosS, which might be attributable to their different autooxidation rates. The different responsiveness of DosS and DosT is caused by the difference in their GAF-A domains accommodating the hemes. The amino acid residues involved in the functional conversion of DosS to DosT were identified.

ACKNOWLEDGMENTS

We thank David Sherman for kindly providing the suicide vector pKO.

This work was supported by a Korean Research Foundation grant (KRF-2008-313-C00779) funded by the Korean government. This study was also supported by Pusan National University (postdoctoral program, 2009).

REFERENCES

1. **Aranda, R., H. Cai, C. E. Worley, E. J. Levin, R. Li, J. S. Olson, G. N. Phillips, and M. P. Richards.** 2009. Structural analysis of fish versus mammalian hemoglobins: effect of the heme pocket environment on autooxidation and hemin loss. Proteins **75:**217–230.
2. **Bartek, I. L., R. Rutherford, V. Gruppo, R. A. Morton, R. P. Morris, M. R. Klein, K. C. Visconti, G. J. Ryan, G. K. Schoolnik, A. Lenaerts, and M. I. Voskuil.** 2009. The DosR regulon of *M. tuberculosis* and antibacterial tolerance. Tuberculosis **89:**310–316.
3. **Boon, C., R. Li, R. Qi, and T. Dick.** 2001. Proteins of *Mycobacterium bovis* BCG induced in the Wayne dormancy model. J. Bacteriol. **183:**2672–2676.
4. **Brantley, R. E., S. J. Smerdon, A. J. Wilkinson, E. W. Singleton, and J. S. Olson.** 1993. The mechanism of autooxidation of myoglobin. J. Biol. Chem. **268:**6995–7010.

5. **Cho, H. Y., H. J. Cho, Y. M. Kim, J. I. Oh, and B. S. Kang.** 2009. Structural insight into the heme-based redox sensing by DosS from *Mycobacterium tuberculosis*. J. Biol. Chem. **284:**13057–13067.
6. **Converse, P. J., P. C. Karakousis, L. G. Klinkenberg, A. K. Kesavan, L. H. Ly, S. S. Allen, J. H. Grosset, S. K. Jain, G. Lamichhane, Y. C. Manabe, D. N. McMurray, E. L. Nuermberger, and W. R. Bishai.** 2009. Role of the *dosR-dosS* two-component regulatory system in *Mycobacterium tuberculosis* virulence in three animal models. Infect. Immun. **77:**1230–1237.
7. **Cunningham, A. F., and C. L. Spreadbury.** 1998. Mycobacterial stationary phase induced by low oxygen tension: cell wall thickening and localization of the 16-kilodalton alpha-crystallin homolog. J. Bacteriol. **180:**801–808.
8. **Dasgupta, N., V. Kapur, K. K. Singh, T. K. Das, S. Sachdeva, K. Jyothisri, and J. S. Tyagi.** 2000. Characterization of a two component system, *devR-devS*, of *Mycobacterium tuberculosis*. Tuber. Lung Dis. **80:**141–159.
9. **Desjardin, L. E., L. G. Hayes, C. D. Sohaskey, L. G. Wayne, and K. D. Eisenach.** 2001. Microaerophilic induction of the alpha-crystallin chaperone protein homologue (*hspX*) mRNA of *Mycobacterium tuberculosis*. J. Bacteriol. **183:**5311–5316.
10. **Florczyk, M. A., L. A. McCue, R. F. Stack, C. R. Hauer, and K. A. McDonough.** 2001. Identification and characterization of mycobacterial proteins differentially expressed under standing and shaking culture conditions, including Rv2623 from a novel class of putative ATP-binding proteins. Infect. Immun. **69:**5777–5785.
11. **Honaker, R. W., R. L. Leistikow, I. L. Bartek, and M. I. Voskuil.** 2009. Unique roles of DosT and DosS in DosR regulon induction and *Mycobacterium tuberculosis* dormancy. Infect. Immun. **77:**3258–3263.
12. **Howard, N. S., J. E. Gomez, C. Ko, and W. R. Bishai.** 1995. Color selection with a hygromycin-resistance-based *Escherichia coli*-mycobacterial shuttle vector. Gene **166:**181–182.
13. **Ioanoviciu, A., Y. T. Meharenna, T. L. Poulos, and P. R. O. de Montellano.** 2009. DevS oxy complex stability identifies this heme protein as a gas sensor in *Mycobacterium tuberculosis* dormancy. Biochemistry **48:**5839–5848.
14. **Ioanoviciu, A., E. T. Yukl, P. Moenne-Loccoz, and P. R. O. de Montellano.** 2007. DevS, a heme-containing two-component oxygen sensor of *Mycobacterium tuberculosis*. Biochemistry **46:**4250–4260.
15. **Jessee, J.** 1986. New subcloning efficiency competent cells: $>1\times10^6$ transformants/μg. Focus **8:**9.
16. **Kendall, S. L., F. Movahedzadeh, S. C. G. Rison, L. Wernisch, T. Parish, K. Duncan, J. C. Betts, and N. G. Stoker.** 2004. The *Mycobacterium tuberculosis dosRS* two-component system is induced by multiple stresses. Tuberculosis **84:**247–255.
17. **Kumar, A., J. C. Toledo, R. P. Patel, J. R. Lancaster, and A. J. C. Steyn.** 2007. *Mycobacterium tuberculosis* DosS is a redox sensor and DosT is a hypoxia sensor. Proc. Natl. Acad. Sci. U. S. A. **104:**11568–11573.
18. **Lee, J. M., H. Y. Cho, H. J. Cho, I. J. Ko, S. W. Park, H. S. Baik, J. H. Oh, C. Y. Eom, Y. M. Kim, B. S. Kang, and J. I. Oh.** 2008. O_2- and NO-sensing mechanism through the DevSR two-component system in *Mycobacterium smegmatis*. J. Bacteriol. **190:**6795–6804.
19. **Leistikow, R. L., R. A. Morton, I. L. Bartek, I. Frimpong, K. Wagner, and M. I. Voskuil.** 2010. The *Mycobacterium tuberculosis* DosR regulon assists in metabolic homeostasis and enables rapid recovery from nonrespiring dormancy. J. Bacteriol. **192:**1662–1670.
20. **Mayuri, G. Bagchi, T. K. Das, and J. S. Tyagi.** 2002. Molecular analysis of the dormancy response in *Mycobacterium smegmatis*: expression analysis of genes encoding the DevR-DevS two-component system, Rv313c and chaperone alpha-crystallin homologues. FEMS Microbiol. Lett. **211:**231–237.
21. **Muttucumaru, D. G. N., G. Roberts, J. Hinds, R. A. Stabler, and T. Parish.** 2004. Gene expression profile of *Mycobacterium tuberculosis* in a non-replicating state. Tuberculosis **84:**239–246.
22. **Oelmuller, U., N. Kruger, A. Steinbuchel, and C. G. Friedrich.** 1990. Isolation of procaryotic RNA and detection of specific mRNA with biotinylated probes. J. Microbiol. Methods **11:**12.
23. **O'Toole, R., M. J. Smeulders, M. C. Blokpoel, E. J. Kay, K. Lougheed, and H. D. Williams.** 2003. A two-component regulator of universal stress protein expression and adaptation to oxygen starvation in *Mycobacterium smegmatis*. J. Bacteriol. **185:**1543–1554.
24. **Park, H. D., K. M. Guinn, M. I. Harrell, R. Liao, M. I. Voskuil, M. Tompa, G. K. Schoolnik, and D. R. Sherman.** 2003. Rv3133c/*dosR* is a transcription factor that mediates the hypoxic response of *Mycobacterium tuberculosis*. Mol. Microbiol. **48:**833–843.
25. **Podust, L. M., A. Ioanoviciu, and P. R. O. de Montellano.** 2008. 2.3 angstrom X-ray structure of the heme-bound GAF domain of sensory histidine DosT of *Mycobacterium tuberculosis*. Biochemistry **47:**12523–12531.
26. **Roberts, D. M., R. L. P. Liao, G. Wisedchaisri, W. G. J. Hol, and D. R. Sherman.** 2004. Two sensor kinases contribute to the hypoxic response of *Mycobacterium tuberculosis*. J. Biol. Chem. **279:**23082–23087.
27. **Rustad, T. R., M. I. Harrell, R. Liao, and D. R. Sherman.** 2008. The enduring hypoxic response of *Mycobacterium tuberculosis.* PLoS One **3:**e1502. 18231589.
28. **Rustad, T. R., A. M. Sherrid, K. J. Minch, and D. R. Sherman.** 2009. Hypoxia: a window into *Mycobacterium tuberculosis* latency. Cell. Microbiol. **11:**1151–1159.
29. **Saini, D. K., V. Malhotra, D. Dey, N. Pant, T. K. Das, and J. S. Tyagi.** 2004. DevR-DevS is a bona fide two-component system of *Mycobacterium tuberculosis* that is hypoxia-responsive in the absence of the DNA-binding domain of DevR. Microbiology **150:**865–875.
30. **Saini, D. K., V. Malhotra, and J. S. Tyagi.** 2004. Cross talk between DevS sensor kinase homologue, Rv2027c, and DevR response regulator of *Mycobacterium tuberculosis*. FEBS Lett. **565:**75–80.
31. **Sambrook, J., and D. Russell.** 2001. Molecular cloning: a laboratory manual, 3rd ed. Cold Spring Harbor Laboratory Press, Cold Spring Harbor, NY.
32. **Sardiwal, S., S. L. Kendall, F. Movahedzadeh, S. C. G. Rison, N. G. Stoker, and S. Djordjevic.** 2005. A GAF domain in the hypoxia/NO-inducible *Mycobacterium tuberculosis* DosS protein binds haem. J. Mol. Biol. **353:**929–936.
33. **Sheffield, P., S. Garrard, and Z. Derewenda.** 1999. Overcoming expression and purification problems of RhoGDI using a family of "parallel" expression vectors. Protein Expr. Purif. **15:**34–39.
34. **Sherman, D. R., M. Voskuil, D. Schnappinger, R. L. Liao, M. I. Harrell, and G. K. Schoolnik.** 2001. Regulation of the *Mycobacterium tuberculosis* hypoxic response gene encoding alpha-crystallin. Proc. Natl. Acad. Sci. U. S. A. **98:**7534–7539.
35. **Snapper, S. B., R. E. Melton, S. Mustafa, T. Kieser, and W. R. Jacobs.** 1990. Isolation and characterization of efficient plasmid transformation mutants of *Mycobacterium smegmatis*. Mol. Microbiol. **4:**1911–1919.
36. **Sousa, E. H. S., J. R. Tuckerman, G. Gonzalez, and M. A. Gilles-Gonzalez.** 2007. DosT and DevS are oxygen-switched kinases in *Mycobacterium tuberculosis*. Protein Sci. **16:**1708–1719.
37. **Starck, J., G. Kallenius, B. I. Marklund, D. I. Andersson, and T. Akerlund.** 2004. Comparative proteome analysis of *Mycobacterium tuberculosis* grown under aerobic and anaerobic conditions. Microbiology **150:**3821–3829.
38. **Voskuil, M. I., D. Schnappinger, K. C. Visconti, M. I. Harrell, G. M. Dolganov, D. R. Sherman, and G. K. Schoolnik.** 2003. Inhibition of respiration by nitric oxide induces a *Mycobacterium tuberculosis* dormancy program. J. Exp. Med. **198:**705–713.
39. **Voskuil, M. I., K. C. Visconti, and G. K. Schoolnik.** 2004. *Mycobacterium tuberculosis* gene expression during adaptation to stationary phase and low-oxygen dormancy. Tuberculosis **84:**218–227.
40. **Wayne, L. G., and L. G. Hayes.** 1996. An *in vitro* model for sequential study of shiftdown of *Mycobacterium tuberculosis* through two stages of nonreplicating persistence. Infect. Immun. **64:**2062–2069.
41. **Wayne, L. G., and C. D. Sohaskey.** 2001. Nonreplicating persistence of *Mycobacterium tuberculosis*. Annu. Rev. Microbiol. **55:**139–163.
42. **Yanisch-Perron, C., J. Vieira, and J. Messing.** 1985. Improved M13 phage cloning vectors and host strains: nucleotide sequences of the M13mpl8 and pUC19 vectors. Gene **33:**103–119.
43. **Yuan, Y., D. D. Crane, R. M. Simpson, Y. Q. Zhu, M. J. Hickey, D. R. Sherman, and C. E. Barry.** 1998. The 16-kDa alpha-crystallin (Acr) protein of *Mycobacterium tuberculosis* is required for growth in macrophages. Proc. Natl. Acad. Sci. U. S. A. **95:**9578–9583.